

Communication

Precise Control of the Preparation of Proton Exchange Membranes via Direct Electrostatic Deposition

Hao Liu ¹, Runmin Tian ¹, Chunxu Liu ¹, Jinghan Zhang ^{1,2}, Mingwei Tian ³ , Xin Ning ^{1,2} , Xingyou Hu ^{1,*} and Hang Wang ^{1,2,*}

¹ Industrial Research Institute of Nonwovens & Technical Textiles, College of Textiles & Clothing, Qingdao University, Qingdao 266071, China

² Shandong Special Nonwoven Materials Engineering Research Center, Qingdao University, Qingdao 266071, China

³ State Key Laboratory of Bio-Fibers and Eco-Textiles, Qingdao University, Qingdao 266071, China

* Correspondence: huxingyou@qdu.edu.cn (X.H.); wanghang@qdu.edu.cn (H.W.)

Abstract: In this work, we reported a novel preparation method for a proton exchange membrane (PEM) named, the direct electrostatic deposition method. In theory, any required thickness and size of PEM can be precisely controlled via this method. By direct electrostatic spraying of Nafion solution containing amino modified SiO₂ nanoparticles onto a metal collector, a hybrid membrane of 30 μm thickness was fabricated. The DMFC assembled with a prepared ultrathin membrane showed a maximum power density of 124.01 mW/cm² at 40 °C and 100% RH, which was 95.29% higher than that of Nafion. This membrane formation method provides potential benefits for the preparation of ultrathin PEMs.

Keywords: direct electrostatic deposition; proton exchange membrane; direct methanol fuel cell; ultrathin membrane; high power density



Citation: Liu, H.; Tian, R.; Liu, C.; Zhang, J.; Tian, M.; Ning, X.; Hu, X.; Wang, H. Precise Control of the Preparation of Proton Exchange Membranes via Direct Electrostatic Deposition. *Polymers* **2022**, *14*, 3975. <https://doi.org/10.3390/polym14193975>

Academic Editors: Yang Zhou and Zhaoling Li

Received: 25 July 2022

Accepted: 18 September 2022

Published: 23 September 2022

Publisher's Note: MDPI stays neutral with regard to jurisdictional claims in published maps and institutional affiliations.



Copyright: © 2022 by the authors. Licensee MDPI, Basel, Switzerland. This article is an open access article distributed under the terms and conditions of the Creative Commons Attribution (CC BY) license (<https://creativecommons.org/licenses/by/4.0/>).

1. Introduction

The use of fossil fuels brings about tremendous problems for resources and the environment, such as greenhouse effects, acid rain, ozone depletion, etc. [1,2]. Among them, greenhouse effects have caused concern around the world due to their serious effect on the environment and climate. Global decarbonization is of great importance, and China has put forward its carbon-neutral strategy [3]. Therefore, the research and development of new energy conversion devices will be vigorously promoted. However, it is difficult to apply renewable energy sources (such as solar energy and wind energy) continuously and stably due to their instability and intermittence during generation [4]. To tackle this issue, the employment of electrochemical energy storage systems, especially direct methanol fuel cells (DMFCs), has received wide attention throughout the world [5–8]. In the future, they will play a major role in improving energy efficiency and reducing fossil fuels. In DMFC components, proton exchange membranes (PEMs) act as proton-conductive mediums for protons as well as barriers for the passage of electrons and fuels between the anode and cathode components [9–12]. PEM is one of the key components which can directly affect the performance of DMFCs. Perfluorinated sulfonic acid resin, such as Nafion from Dupont, has been widely used as the PEM in DMFC because of its excellent chemical stability, and good mechanical strength derived from the hydrophobic PTFE backbone. Furthermore, the ionic domains formed between the hydrophilic-SO₃H in the side chain and the hydrophobic PTFE backbone in the Nafion structure could provide good proton conductivity ($\geq 0.1 \text{ S cm}^{-1}$), which ensures its practical applications [13]. However, some drawbacks, such as high cost, high methanol permeability, and low proton conductivity under low humidity conditions, drastically limit the widespread commercial application of Nafion in fuel cells.

Recently, nanocomposites have raised a lot of research interest in the preparation of PEMs due to the significant improvement in performance based on the nature of nanomaterials, including nanoparticles, nanowires, nanofibers, nanosheets, etc. [14,15]. Among these nanomaterials, silica has attracted the greatest interest due to its high specific surface area and convenient surface modification. Much literature has proved that the addition of inorganic silica to PEM polymers can improve thermal stability, proton conductivity as well as methanol resistance [16]. Zhao et al. [17] prepared composite PEMs by doping amino-functionalized mesoporous silica (AMS) with SP/IL (N-ethylimidazole trifluoromethanesulfonate) and found that amino-functionalized mesoporous silica contributed to the proton transfer due to large lumen channels and acid–base pairs between $-\text{NH}_2$ and $-\text{SO}_3\text{H}$. The prepared composite membrane with AMS reached a high proton conductivity of 1.494 mS/cm under anhydrous conditions at 200 °C, which is four times that of the composite membrane with pure silica. Mahdavi et al. [18] presented a novel nanocomposite PEM containing sulfonated polysulfone, metal–organic frameworks and silica nanoparticles. The combination of silica nanoparticles and MOFs in a matrix can act as proton hopping sites to enhance the transport efficiency of protons. Results showed that the prepared PEMs containing 5% nanoparticles demonstrated a high proton conductivity of 17 mS/cm at 70 °C and a maximum power density of 40.80 mW/cm². These experiments proved that functional silica is of great significance to the performance of PEMs.

Nowadays, the strategies and techniques for the preparation of PEM mainly include recasting or blending [19–21], hot-pressing [22,23] and impregnation [24–27]. Recasting is a simple and low-cost membrane formation method that can offer easy optimization of the processing parameters. The primary requirement for this method is to have the materials well-dissolved in the solvent to ensure the solution is uniform and homogeneous. Hot-pressing is a method for preparing PEMs by means of the difference in melting temperatures of poly-materials. The dense membrane can be prepared by this method only at high temperatures and pressure. Ballengee [28] prepared composite PEMs via hot pressing (127 °C and 15,000 psi) and annealing (from 130 °C to 250 °C). In this process, melted Nafion flowed into the void space between the polyphenylsulfone nanofibers to create a fully dense membrane structure. As the name suggests, the impregnation method refers to incorporating porous materials in a polymer matrix to form a dense membrane [29]. Similar to hot-pressing, the impregnated membrane is prepared by filling voids of porous materials with the polymer matrix solution. The nanofiber composite membranes are frequently prepared using this route. These methods have their own advantages; however, the precise control of the preparation process and the preparation of ultrathin composite membranes still remain major challenges for them. However, the membrane size and thickness can only be controlled by the volume of the casting solution roughly.

Recently, the direct membrane formation method has been reported for simplifying and optimizing the fabrication process of MEAs. Klingele et al. [30] directly deposited a Nafion[®] dispersion onto gas diffusion electrodes with catalyst layers as membrane layers, and then pressed two electrodes together with the membrane layers facing each other. This approach constructed the relatively thinner PEM in MEAs to strongly decrease the contact resistance of the membrane and the proton conducting phase of the catalyst layer. Their directly deposited MEAs demonstrated a high power density up to 4.07 W/cm² under H₂/O₂ single cell performance test. Breitwieser et al. [31] presented a novel method of MEA preparation by combining scalable deposition and electrospinning to achieve the manufacturing of MEAs with a controlled 3D design; the fabricated composite membranes showed an ultra-thin thickness of 12 μm. These studies demonstrated deposition can improve the freedom degrees of complex MEAs design.

In this work, we present a novel membrane preparation technology of direct electrostatic deposition (DED), where the membrane is directly prepared on a substrate via electrostatic spraying, which is similar to the electrospinning technology. In this process, the polymer solution was sprayed onto a substrate via a spinneret which has a hole diameter of 0.1 mm. With the solution solidified layer by layer under high-temperature

treatment of a substrate, the thickness of the membrane increased at a very slow rate; then the robust and continuous membrane formed. Depending on the increase in thickness on the nanometer scale, the thickness of the membrane can be controlled precisely and simply by spraying time and spraying rate. Besides, the size of the membrane can be precisely controlled by the operation track. Considering the weak proton conductivity of pure SiO_2 nanospheres, amino groups ($-\text{NH}_2$) were introduced on their surface to improve compatibility and conduction. More importantly, amino groups in nanomaterials and acid groups in the matrix can form acid–base pairs to accelerate proton transfer. Therefore, we introduced amino-modified SiO_2 nanoparticles ($\text{SiO}_2\text{--NH}_2$) into Nafion to prepare the hybrid PEM by DED. The schematic workflow of the preparation of the PEM is shown in Figure 1. Furthermore, the DMFC single cell performance of the as-prepared membrane and Nafion membrane was investigated.

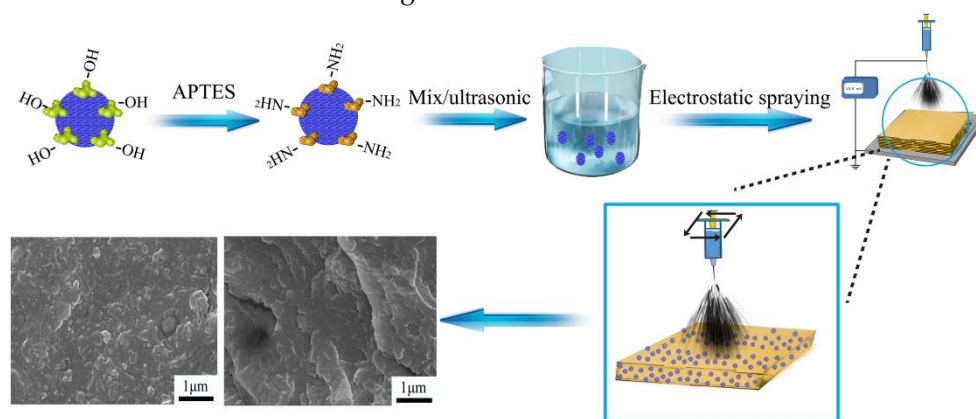


Figure 1. The schematic workflow of the preparation of the PEM.

2. Materials and Methods

2.1. Preparation of the Hybrid Membrane

The detailed synthetic method of $\text{SiO}_2\text{--NH}_2$ referred to the published literature [32]. Ethanol was chosen as the solvent due to its low boiling point advantage. A certain amount of $\text{SiO}_2\text{--NH}_2$ nanoparticles and Nafion solution (5%) were successively dispersed in ethanol to obtain a silica/Nafion suspension. Herein, the percent of silica and Nafion in suspension was 0.15% and 2.5%, respectively, and the total fraction of $\text{SiO}_2\text{--NH}_2$ in the final membrane without solvent was approximately 5.7%. Then the final suspension with Nafion and $\text{SiO}_2\text{--NH}_2$ underwent ultrasonic treatment for 2 h to break the aggregates. For electro spraying, an electrostatic painting instrument equipped with a solution extrusion device, liquid injection needle, voltage system and heating metal collector was used. The process parameters of hybrid membrane preparation were 1 kV voltage, a tip collector distance of 2 cm, an operation track of $5\text{ cm} \times 5\text{ cm}$, a spray rate of 0.1 and 0.15 mL/min and a collector temperature of $75\text{ }^\circ\text{C}$. To compare the single cell performances in DMFC, the prepared hybrid membrane with a thickness of $30\text{ }\mu\text{m}$ was prepared and designed as Nafion/ $\text{SiO}_2\text{--NH}_2$ in this work. All membranes were impregnated in $2\text{ M H}_2\text{SO}_4$ for 12 h and washed with deionized water until neutralized.

2.2. Characterization

Scanning electron microscopy (SEM, Hitachi S-4800) and transmission electron microscopy (TEM, JEM 2200FS) were used to observe the morphologies of samples. Energy-dispersive X-ray spectra (EDS) mapping and X-ray photoelectron spectroscopy (XPS) were used to examine the composition of $\text{SiO}_2\text{--NH}_2$. Wide-angle X-ray diffractometry (XRD) and small-angle X-ray scattering (SAXS) measurements were carried out using an X-ray diffractometer (Rigaku SmartLab SE, Japan) and an Anton Paar SAXS system (SAXS ess mc2, Austria), respectively.

Proton conductivity (σ) was measured by AC impedance spectroscopy using an electrochemical workstation under a heated water bath. The frequency range from 0.1 to 10^5 Hz σ was calculated using the following equation:

$$\sigma = L/(R \cdot A) \quad (1)$$

where L , R , and A are the electrode distance, the impedance, and the membrane cross-sectional area, respectively.

The methanol permeability was measured via a diffusion cell containing two glass compartments sandwiching the test sample. The methanol permeability was calculated through the following equation:

$$DK = \frac{L \cdot V_B \cdot C_{B(t)}}{A \cdot C_{A(t-t_0)}} \quad (2)$$

where DK is the methanol permeability; L , A , and V_B correspond to the thickness of the membrane, the effective area, and the volume of the water side, respectively; C_A and C_B are the concentration of methanol (M) in the A side and B side, which can be monitored by gas chromatography (Agilent 7820); $t - t_0$ is the test time.

The MEA was prepared by (i) spraying the anode catalyst (PtRu/C, Pt:Ru = 1:1, Johnson Matthey) and cathode catalyst (Pt/C, 60% Pt, Johnson Matthey, London, UK) on the PEM layer (2 cm \times 2 cm), and both the catalyst loading was 1 mg/cm²; (ii) Sandwiching the above membrane with gas diffusion layers and hot pressing at 100 °C. The DMFC performances of membrane electrode assemblies (MEAs) with different membranes were characterized by polarization curves in a fuel cell testing station (Model TEID160-1NBNNS, Arbin Inc., College Station, TX, USA) at 40 °C. The aqueous methanol (2 M) and oxygen were fed to the anode and cathode at 2 mL/min and 500 mL/min, respectively.

3. Results and Discussion

3.1. Characterization of SiO₂-NH₂

SEM, TEM-EDS mapping and XPS tests were used to characterize the morphology and elemental composition of SiO₂-NH₂. It could be seen in Figure 2a that the SiO₂-NH₂ we synthesized showed a well-defined spherical appearance, and possessed a rough surface caused by the aggregation of -NH₂. As shown in Figure 2b, N, O and Si elements are uniformly distributed in the nanoparticles, which demonstrates the successful synthesis of the SiO₂-NH₂. In addition, the peaks of O (1s), N (1s), C (1s), Si (2s) and Si (2p) shown in Figure 2c could further prove the successful preparation of SiO₂-NH₂. Furthermore, the elemental analysis of SiO₂-NH₂ by XPS confirmed the Nitrogen percentage of 1.45%, which corresponds to 1.66% of -NH₂.

3.2. Characterization of Nafion/SiO₂-NH₂

The realization of DED via electrostatic spraying mainly depends on the electric force and high-temperature solidification. The membrane fabrication process can be divided into two stages. In the first stage, the surface tension and viscoelastic force of membrane solution are overcome by the electric force, and then spraying type jets are formed and deposited on the collector. Different from the electrospinning process, solvent evaporation during spraying is extremely slow due to the short distance and relatively low voltage. In the second stage, the solution deposited on the collector solidifies to the membrane rapidly because of the high temperature.

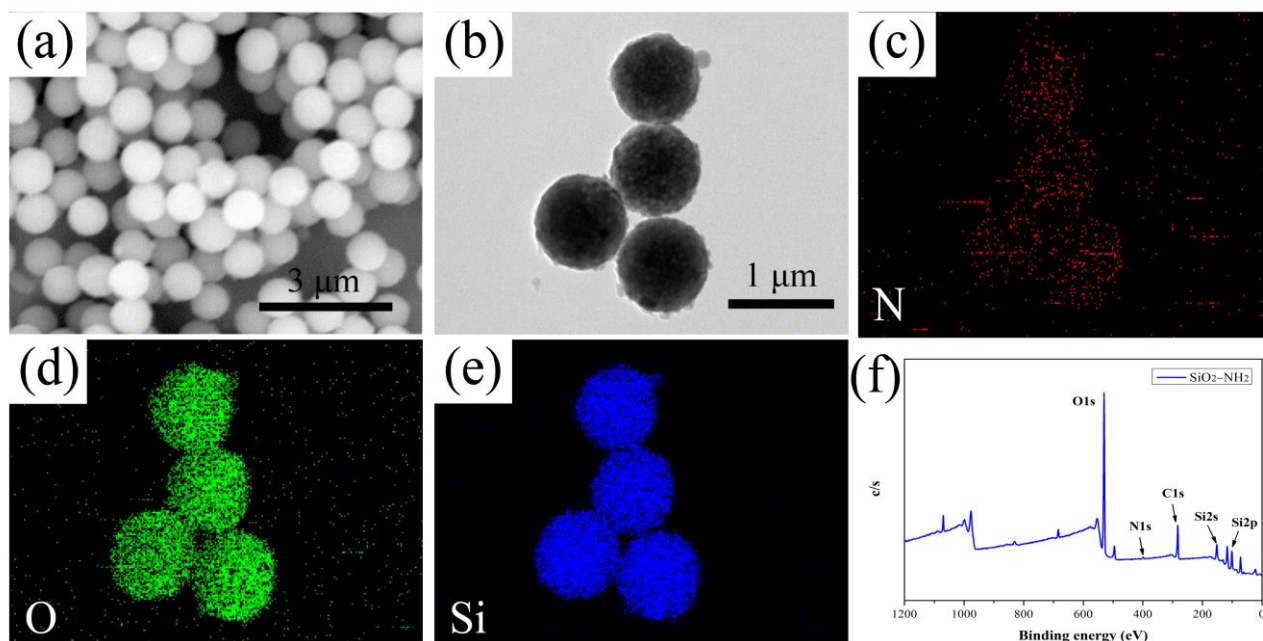


Figure 2. (a) SEM, (b–e) TEM-EDS mapping and (f) XPS images of $\text{SiO}_2\text{-NH}_2$.

The thickness of the composite membranes changed with the spraying time and spraying rate as shown in Figure 3. The thickness of the membrane shows a linearly increasing trend with the increased spraying time. Moreover, the thickness of the membrane prepared by a spraying rate of 0.15 mL/min is larger than that of the membrane with a spraying rate of 0.1 mL/min. In particular, the error bars of membrane thickness is quite small. Therefore, a membrane with a certain thickness and size can be prepared on a large scale using DED. The above phenomenon shows that the thickness of the membrane prepared by DED can be precisely controlled by spraying time and spraying rate.

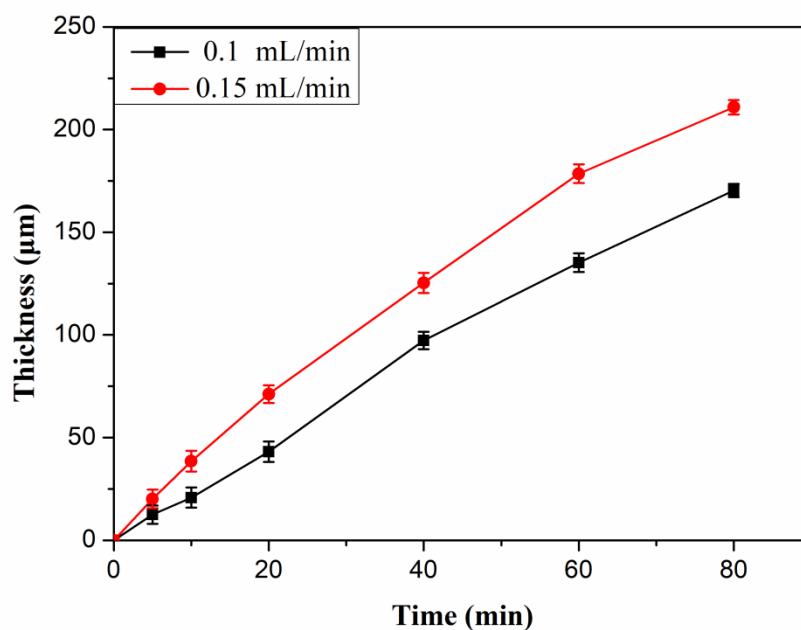


Figure 3. The thickness-time relationship at spraying rates of 0.1 and 0.15 mL/min.

Morphology of the Nafion/ $\text{SiO}_2\text{-NH}_2$: SEM images of the surface and cross-sectional hybrid membranes at different magnifications are shown in Figure 4. As shown in Figure 4, the surface and cross-section of Nafion/ $\text{SiO}_2\text{-NH}_2$ is compact, and no significant crack

is shown in the membrane. Furthermore, the SiO₂-NH₂ nanoparticles could be clearly observed at both their surface and cross-section. This result revealed the good dispersion of SiO₂-NH₂ in the Nafion matrix.

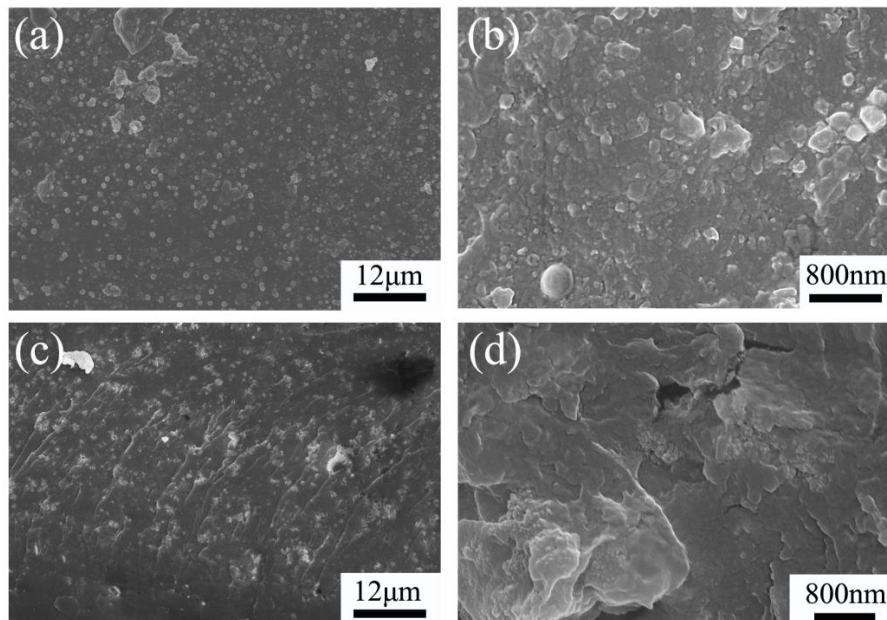


Figure 4. (a,b) the surface and (c,d) cross-sectional SEM images of hybrid membranes at different magnifications.

Figure 5a shows the XRD patterns of Nafion, Nafion/SiO₂-NH₂ and SiO₂-NH₂. All the samples showed amorphous peaks, indicating amorphous characteristics. Comparing the XRD patterns of Nafion/SiO₂-NH₂ with Nafion, a new broad peak appeared for the composite membranes at 24°. This result is caused by the redistribution of SiO₂-NH₂ in the Nafion matrix and reveals the good compatibility of these components.

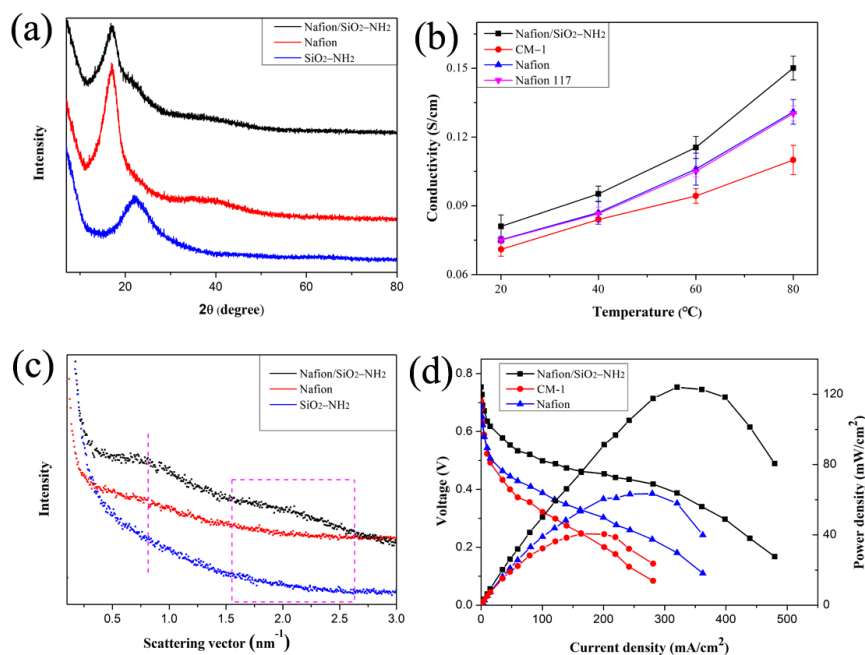


Figure 5. (a) XRD curves of Nafion, Nafion/SiO₂-NH₂ and SiO₂-NH₂; (b) Proton conductivity curve, (c) SAXS curves and (d) DMFC performance (operated at 40 °C and 100% RH) of Nafion/SiO₂-NH₂, Nafion and CM-1.

The proton conductivity of commercial Nafion 117, pure Nafion and hybrid Nafion membrane prepared by DED is shown in Figure 5b. Pure Nafion exhibited similar proton conductivity with Nafion 117 indicating the processing reliability of DED in membrane formation. The compared membrane containing the same content of SiO₂-NH₂ and Nafion matrix are prepared by the casting method and named CM-1. It is interesting that CM-1 showed lower proton conductivity than Nafion/SiO₂-NH₂ and Nafion. Nevertheless, Nafion/SiO₂-NH₂ exhibited the highest proton conductivity of 0.15 S/cm at 80 °C. This difference in proton conductivity originated from the different microstructure; better distribution of SiO₂-NH₂ in a hybrid membrane could bridge ionic clusters in the membrane to form continuous proton transferred channels [33]. During the casting process, nanospheres tend to be distributed on one side of the membrane, affected by gravity. However, high temperature facilitated the micro-volume polymer solution spinneret from solidification on the collector and then formed a layer-by-layer membrane with a homogeneous nanocomposite structure. This conclusion could be verified by the results of cross-sectional SEM images of hybrid membranes. To better verify the above explanation, SAXS of all membranes were characterized (Figure 5c). Nafion/SiO₂-NH₂ showed an obvious matrix segment peak and ionomer peak at lower and higher *q*, respectively. However, the peaks of CM-1 and pure Nafion were not obvious. Based on Bragg's law, the distance between neighboring ionic clusters in Nafion/SiO₂-NH₂ was smaller than in other membranes [34]. Such an observation is also consistent with the proton conductivity results.

Table 1 shows the methanol permeability of Nafion, Nafion/SiO₂-NH₂, and CM-1. Compared with the Nafion membrane, Nafion/SiO₂-NH₂ exhibited lower methanol permeability, indicating that the introduction of SiO₂ improves the methanol barrier properties. However, the methanol permeability of CM-1 is lower compared to Nafion/SiO₂-NH₂, probably because of the reunion distribution of inorganic particles on one side of the membrane to form methanol barrier layers. This result is consistent with the proton conductivity results.

Table 1. The methanol permeability of Nafion, Nafion/SiO₂-NH₂, and CM-1.

Samples	Methanol Permeability (10 ⁻⁷ cm ² s ⁻¹)
Nafion	17.5
Nafion/SiO ₂ -NH ₂	9.8
CM-1	9.1

The polarization and performance curves of passive DMFCs based on pure Nafion and hybrid Nafion/SiO₂-NH₂ membranes were collected at 40 °C and 100% RH and are shown in Figure 5c. It can be seen from Figure 5c that the DMFC performance of Nafion/SiO₂-NH₂ is enhanced compared to that of Nafion. Particularly, Nafion/SiO₂-NH₂ had a maximum power density output of 124.01 mW/cm². However, Nafion and CM-1 only showed maximum power density values of 63.50 and 40.60 mW/cm², respectively. This result is likely due to the following aspects: (i) the ultrathin Nafion/SiO₂-NH₂ can transport protons effectively through the membrane; (ii) the well-distributed inorganic silica may improve the water retention and methanol permeability of Nafion; (iii) the more ionic clusters in Nafion/SiO₂-NH₂ can provide massive proton transfer sites.

Some published works related to inorganic/organic hybrid membranes were cited for comparison with proton conductivity and power density, as shown in Table 2. The proton conductivity and power density for Nafion/SiO₂-NH₂ showed a competitive overall performance than other membranes, verifying that DED is a good application prospect in PEM preparation.

Table 2. Comparison of proton conductivity and power density with other reported PEMs.

PEMs	Proton Conductivity (S/cm)	Power Density (mW/cm ²)	Ref.
PSU/mMOF/Si-SO ₃ H	0.017 (70 °C, 100% RH)	40.8 (70 °C)	[18]
SPEEK/TiNFs-1.0	0.037 (80 °C, 100% RH)	431.5 (60 °C)	[35]
SPEEK/S-SiO ₂ /MOF-5	0.00369 (30 °C, 100% RH)	NA	[36]
Nafion/SPES/SiO ₂ -3%	0.23 (80 °C, 100% RH)	77.22 (80 °C)	[37]
Nafion/SiO ₂ -NH ₂	0.15 (80 °C, 100% RH)	124.01 (40 °C)	This work

4. Conclusions

A novel approach to precisely control the fabrication of PEMs for DMFCs operating was presented in this work. Nafion/SiO₂-NH₂ was directly formed on a metal collector enabling the fast, simple and precise fabrication of 30 μm thin composite membranes. Nafion/SiO₂-NH₂ showed a maximum power density of 124.01 mW/cm² at 40 °C and 100% RH, which was 95.29% higher than that of Nafion. The results proved that the DED can be a potential method for the precise production of cost-effective and ultrathin membranes.

Author Contributions: Conceptualization, H.L., J.Z. and H.W.; methodology, H.L., J.Z. and H.W.; validation, R.T., C.L. and X.H.; formal analysis, H.L., J.Z., R.T., C.L., X.H. and H.W.; investigation, H.W.; resources, H.W.; data curation, H.L., J.Z. and H.W.; writing—original draft preparation, J.Z. and H.W.; writing—review and editing, H.L. and H.W.; supervision, H.W., M.T. and X.N.; project administration, H.W. All authors have read and agreed to the published version of the manuscript.

Funding: This work was funded by Natural Science Foundation of Shandong Province of China (ZR2020QE074 and ZR2021QC112), the China Postdoctoral Science Fund (NO. 2020M671996), Shandong provincial universities youth innovation technology plan innovation team (2020KJA013), and Student Innovation and Entrepreneurship Training Program of Qingdao University (X2021110650106 and X2021110650158).

Institutional Review Board Statement: Not applicable.

Informed Consent Statement: Not applicable.

Data Availability Statement: The data presented in this study are available on request from the corresponding author.

Conflicts of Interest: The authors declare no conflict of interest.

References

- Elwan, H.; Mamlouk, M.; Scott, K. A review of proton exchange membranes based on protic ionic liquid/polymer blends for polymer electrolyte membrane fuel cells. *J. Power Sources* **2021**, *484*, 229197. [CrossRef]
- Whiting, K.; Carmona, L.; Sousa, T. A review of the use of exergy to evaluate the sustainability of fossil fuels and non-fuel mineral depletion. *Renew. Sustain. Energy Rev.* **2017**, *76*, 202–211. [CrossRef]
- Vinothkannan, M.; Kim, A.; Ramakrishnan, S.; Yu, Y.; Yoo, D. Advanced Nafion nanocomposite membrane embedded with unzipped and functionalized graphite nanofibers for high-temperature hydrogen-air fuel cell system: The impact of filler on power density, chemical durability and hydrogen permeability of membrane. *Compos. Part B Eng.* **2021**, *215*, 108828. [CrossRef]
- Sun, C.; Zhang, H. Review of the Development of First-Generation Redox Flow Batteries: Iron-Chromium System. *ChemSusChem* **2022**, *15*, e202101798. [CrossRef] [PubMed]
- Wu, J.; Nie, S.; Liu, H.; Gong, C.; Zhang, Q.; Xu, Z.; Liao, G. Design and development of nucleobase modified sulfonated poly(ether ether ketone) membranes for high-performance direct methanol fuel cells. *J. Mater. Chem. A* **2022**. [CrossRef]
- Huang, H.; Ma, Y.; Jiang, Z. Spindle-like MOFs-derived porous carbon filled sulfonated poly(ether ether ketone): A high performance proton exchange membrane for direct methanol fuel cells. *J. Membr. Sci.* **2021**, *636*, 119585. [CrossRef]
- Simari, C.; Nicotera, I.; Aricò, A.S.; Baglio, V.; Lufrano, F. New insights into properties of methanol transport in sulfonated polysulfone composite membranes for direct methanol fuel cells. *Polymers* **2021**, *13*, 1386. [CrossRef]
- Imaan, D.U.; Mir, F.Q.; Ahmad, B. Synthesis and characterization of a novel poly(vinyl alcohol)-based zinc oxide (PVA-ZnO) composite proton exchange membrane for DMFC. *Int. J. Hydrogen Energy* **2021**, *46*, 12230–12241. [CrossRef]
- Lu, Y.; Liu, Y.; Li, N.; Hu, Z.; Chen, S. Sulfonated graphitic carbon nitride nanosheets as proton conductor for constructing long-range ionic channels proton exchange membrane. *J. Membr. Sci.* **2020**, *601*, 117908. [CrossRef]

10. Imaan, D.U.; Mir, F.Q.; Ahmad, B. In-situ preparation of PSSA functionalized ZWP/sulfonated PVDF composite electrolyte as proton exchange membrane for DMFC applications. *Int. J. Hydrogen Energy* 2022, *in press*. [[CrossRef](#)]
11. Ma, L.; Li, J.; Xiong, J.; Xu, G.; Liu, Z.; Cai, W. Proton conductive channel optimization in methanol resistive hybrid hyperbranched polyamide proton exchange membrane. *Polymers* 2017, *9*, 703. [[CrossRef](#)] [[PubMed](#)]
12. Wang, H.; Zhang, J.; Ning, X.; Tian, M.; Long, Y.; Ramakrishna, S. Recent advances in designing and tailoring nanofiber composite electrolyte membranes for high-performance proton exchange membrane fuel cells. *Int. J. Hydrogen Energy* 2021, *46*, 25225–25251. [[CrossRef](#)]
13. Sun, C.; Zhang, H.; Luo, X.; Chen, N. A comparative study of Nafion and sulfonated poly(ether ether ketone) membrane performance for iron-chromium redox flow battery. *Ionics* 2019, *25*, 4219–4229. [[CrossRef](#)]
14. Zhang, J.; Liu, H.; Ma, Y.; Wang, H.; Chen, C.; Yan, G.; Tian, M.; Long, Y.; Ning, X.; Cheng, B. Construction of dual-interface proton channels based on γ -polyglutamic acid@cellulose whisker/PVDF nanofibers for proton exchange membranes. *J. Power Sources* 2022, *548*, 231981. [[CrossRef](#)]
15. Hyun, J.; Doo, G.; Yuk, S.; Yuk, S.; Lee, D.; Lee, D.; Choi, S.; Kwen, J.; Kang, H.; Tenne, R.; et al. Magnetic Field-Induced Through-Plane Alignment of the Proton Highway in a Proton Exchange Membrane. *ACS Appl. Energy Mater.* 2020, *3*, 4619–4628. [[CrossRef](#)]
16. Sun, C.; Negro, E.; Nale, A.; Pagot, G.; Vezzu, K.; Zawodzinski, T.; Meda, L.; Gambaro, C.; Noto, V. An efficient barrier toward vanadium crossover in redox flow batteries: The bilayer [Nafion/(WO₃)_x] hybrid inorganic-organic membrane. *Electrochim. Acta* 2021, *378*, 138133. [[CrossRef](#)]
17. Zhang, X.; Yu, S.; Zhu, Q.; Zhao, L. Enhanced anhydrous proton conductivity of SPEEK/IL composite membrane embedded with amino functionalized mesoporous silica. *Int. J. Hydrogen Energy* 2019, *44*, 6148–6159. [[CrossRef](#)]
18. Ahmadian-Alam, L.; Mahdavi, H. A novel polysulfone-based ternary nanocomposite membrane consisting of metal-organic framework and silica nanoparticles: As proton exchange membrane for polymer electrolyte fuel cells. *Renew. Energy* 2018, *126*, 630–639. [[CrossRef](#)]
19. Pal, S.; Mondal, R.; Chatterjee, U. Sulfonated polyvinylidene fluoride and functional copolymer based blend proton exchange membrane for fuel cell application and studies on methanol crossover. *Renew. Energy* 2021, *170*, 974–984. [[CrossRef](#)]
20. Patnaik, P.; Mondal, R.; Sarkar, S.; Choudhury, A.; Chatterjee, U. Proton exchange membrane from the blend of poly(vinylidene fluoride) and functional copolymer: Preparation, proton conductivity, methanol permeability, and stability. *Int. J. Hydrogen Energy* 2022, *in press*. [[CrossRef](#)]
21. Ma, L.; Xu, G.; Li, S.; Ma, J.; Li, J.; Cai, W. Design and optimization of a hyper-branched polyimide proton exchange membrane with ultra-high methanol-permeation resistivity for direct methanol fuel cells applications. *Polymers* 2018, *10*, 1175. [[CrossRef](#)] [[PubMed](#)]
22. Sun, L.; Gu, Q.; Wang, H.; Yu, J.; Zhou, X. Anhydrous proton conductivity of electrospun phosphoric acid-doped PVP-PVDF nanofibers and composite membranes containing MOF fillers. *RSC Adv.* 2021, *11*, 29527–29536. [[CrossRef](#)]
23. Wang, H.; Tang, C.; Zhuang, X.; Cheng, B.; Wang, W.; Kang, W.; Li, H. Novel structure design of composite proton exchange membranes with continuous and through-membrane proton-conducting channels. *J. Power Sources* 2017, *365*, 92–97. [[CrossRef](#)]
24. Sood, R.; Giancola, S.; Donnadio, A.; Zatoń, M.; Donzel, N.; Rozière, J.; Jones, D.J.; Cavaliere, S. Active electrospun nanofibers as an effective reinforcement for highly conducting and durable proton exchange membranes. *J. Membr. Sci.* 2021, *622*, 119037. [[CrossRef](#)]
25. Cheng, G.; Li, Z.; Ren, S.; Han, D.; Xiao, M.; Wang, S.; Meng, Y. A robust composite proton exchange membrane of sulfonated poly (fluorenyl ether ketone) with an electrospun polyimide mat for direct methanol fuel cells application. *Polymers* 2021, *13*, 523. [[CrossRef](#)]
26. Li, H.; Lee, Y.; Lai, J.; Liu, Y. Composite membranes of Nafion and poly(styrene sulfonic acid)-grafted poly(vinylidene fluoride) electrospun nanofiber mats for fuel cells. *J. Membr. Sci.* 2014, *466*, 238–245. [[CrossRef](#)]
27. Liu, G.; Tsen, W.; Wen, S. Sulfonated silica coated polyvinylidene fluoride electrospun nanofiberbased composite membranes for direct methanol fuel cells. *Mater. Des.* 2020, *193*, 108806. [[CrossRef](#)]
28. Ballengee, J.B.; Pintauro, P.N. Preparation of nanofiber composite proton-exchange membranes from dual fiber electrospun mats. *J. Membr. Sci.* 2013, *442*, 187–195. [[CrossRef](#)]
29. Zhao, G.; Xu, X.; Zhao, H.; Shi, L.; Zhuang, X.; Cheng, B.; Yin, Y. Zeolitic imidazolate framework decorated on 3D nanofiber network towards superior proton conduction for proton exchange membrane. *J. Membr. Sci.* 2020, *601*, 117914. [[CrossRef](#)]
30. Klingele, M.; Breitwieser, M.; Zengerle, R.; Thiele, S. Direct deposition of proton exchange membranes enabling high performance hydrogen fuel cells. *J. Mater. Chem. A* 2015, *3*, 11239–11245. [[CrossRef](#)]
31. Breitwieser, M.; Klose, C.; Klingele, M.; Hartmann, A.; Erben, J.; Cho, H.; Kerres, J.; Zengerle, R.; Thiele, S. Simple fabrication of 12 μ m thin nanocomposite fuel cell membranes by direct electrospinning and printing. *J. Power Sources* 2017, *337*, 137–144. [[CrossRef](#)]
32. Wang, H.; Li, X.; Feng, X.; Liu, Y.; Kang, W.; Xu, X.; Zhuang, X.; Cheng, B. Novel proton-conductive nanochannel membranes with modified SiO₂ nanospheres for direct methanol fuel cells. *J. Membr. Sci.* 2018, *22*, 3475–3484. [[CrossRef](#)]
33. Wang, H.; Sun, N.; Zhang, L.; Zhou, R.; Ning, X.; Zhuang, X.; Long, Y.; Cheng, B. Ordered proton channels constructed from deoxyribonucleic acid-functionalized graphene oxide for proton exchange membranes via electrostatic layer-by-layer deposition. *Int. J. Hydrogen Energy* 2020, *45*, 27772–27778. [[CrossRef](#)]

34. Zhang, S.; He, G.; Gong, X.; Zhu, X.; Wu, X.; Sun, X.; Zhao, X.; Li, H. Electrospun nanofiber enhanced sulfonated poly (phthalazinone ether sulfone ketone) composite proton exchange membranes. *J. Membr. Sci.* **2015**, *493*, 58–65. [[CrossRef](#)]
35. Dong, C.; Hao, Z.; Wang, Q.; Zhu, B.; Cong, C.; Meng, X.; Zhou, Q. Facile synthesis of metal oxide nanofibers and construction of continuous proton-conducting pathways in SPEEK composite membranes. *Int. J. Hydrogen Energy* **2017**, *42*, 25388–25400. [[CrossRef](#)]
36. Bisht, S.; Balaguru, S.; Ramachandran, S.K.; Gangasalam, A.; Kweon, J. Proton exchange composite membranes comprising SiO₂, sulfonated SiO₂, and metal–organic frameworks loaded in SPEEK polymer for fuel cell applications. *J. Appl. Polym. Sci.* **2021**, *138*, 50530. [[CrossRef](#)]
37. Wang, H.; Wang, X.; Fan, T.; Zhou, R.; Li, J.; Long, Y.; Zhuang, X.; Cheng, B. Fabrication of electrospun sulfonated poly(ether sulfone) nanofibers with amino modified SiO₂ nanosphere for optimization of nanochannels in proton exchange membrane. *Solid State Ion.* **2020**, *349*, 115300. [[CrossRef](#)]